Analytica Chimica Acta 748 (2012) 89–94

Contents lists available at SciVerse ScienceDirect

Analytica Chimica Acta

journal homepage: www.elsevier.com/locate/aca

Ultrasensitive and facile electrochemical deoxyribonucleic acid biosensor based on the conformational change of the recognition interface

Wei Chen[a,*], Yin-Huan Liu[a], Hong-Na Li[a], Ai-Lin Liu[a], Xin-Hua Lin[a,*], Yuan-Zhong Chen[b,*]

[a] Department of Pharmaceutical Analysis, Fujian Medical University, Fuzhou 350004, China
[b] Union Hospital, Fujian Medical University, Fuzhou 350004, China

HIGHLIGHTS

- A quite simple electrochemical impedance spectroscopic DNA biosensor was introduced.
- The sensing protocol was based on the conformational change of DNA.
- This approach is sensitive with a detection limit of 40 fM.

GRAPHICAL ABSTRACT

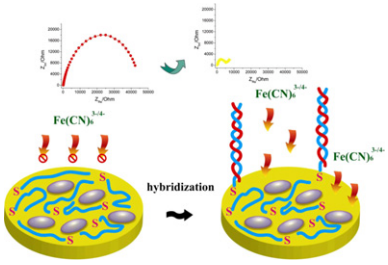

ARTICLE INFO

Article history:
Received 3 June 2012
Received in revised form 21 August 2012
Accepted 28 August 2012
Available online 6 September 2012

Keywords:
Biosensor
Electrochemical impedance spectroscopy
Deoxyribonucleic acid
Conformational change
Recognition interface

ABSTRACT

An ultrasensitive electrochemical impedance spectroscopic deoxyribonucleic acid biosensor has been developed based on the conformational change of the deoxyribonucleic acid recognition interface with lodging probes. Pairing process leads to desorption of deoxyribonucleic acid bases from the gold surface, leading to a significant change of the interfacial conformation and the charge transfer resistance. Remarkably low detection limits down to 40 fM are thus obtained without any additional amplification step.

1. Introduction

In recent years, an impressive number of electrochemical DNA biosensors have been invented and employed to detect specific nucleotide sequences relied on the high specificity of base paring interactions between complementary strands of DNA [1–14]. The high sensitivity of electrochemical transducers, as well as their compatibility with modern microfabrication and miniaturization technologies, small dimensions, low cost and power requirements, and their independence of sample turbidity, makes such devices excellent candidates for DNA diagnosis.

Due to its ability of directly probing the interfacial properties of a modified electrode, electrochemical impedance spectroscopy (EIS) has been rapidly developing as a simple, rapid, label-free, and low-cost tool for studying biorecognition events at the electrode surface, attracting more and more interest in biosensing applications recently [15–17]. However, the sensitivity of EIS biosensor is still a major limitation to its wider application. In this paper, a label-free and quite simple EIS DNA biosensor was introduced. Absolutely different from the conventional strategy, our sensing protocol was based on the conformational change of DNA from flexible single strand to rigid double strand on the gold surface. This strategy is shown to be much more sensitive

* Corresponding authors. Tel.: +86 591 22862016; fax: +86 591 22862016.
E-mail addresses: chenandhu@163.com (W. Chen), xinhua63@163.com (X.-H. Lin), chenyz@pub3.fz.fj.cn (Y.-Z. Chen).

0003-2670/$ – see front matter © 2012 Elsevier B.V. All rights reserved.
http://dx.doi.org/10.1016/j.aca.2012.08.046

Table 1
Oligonucleotide sequences.

Oligonucleotide	Sequence
Probe SH-ssDNA	5′-SH-$(CH_2)_6$-T_{10} CTTCA GAACT GCTGC TCTGG GTCTC AATGG-3′
Target ssDNA	5′-CCATT GAGAC CCAGA GCAGC AGTTC TGAAG-3′
One-base mismatch DNA	5′-CCATT GAGAC CCAGA GCAGC AGTTG TGAAG-3′
Non-complementary DNA	5′-AGTCG CTATG GGTCT CTTAG TCGGA AACCT-3′

than conventional EIS DNA biosensor, with a detection limit of 40 fM.

2. Experimental

2.1. Materials

Chemicals were obtained from either Sigma or Aldrich and used as received, unless otherwise stated. Aqueous solutions were prepared with Milli Q water (18 MΩ cm resistivity) from a Millipore system. A solution of $K_3Fe(CN)_6$ and $K_4Fe(CN)_6$, 4 mM in each component, prepared in 0.1 M KCl, was used for electrochemical impedance spectroscopy measurements. All synthetic oligonucleotides used were purchased from TaKaRa Biotechnology (Dalian, China) and are listed in Table 1. The buffer solutions used in this study were as follows: the DNA immobilization buffer contained 10 mM Tris–HCl, 1 mM EDTA, and 1 M NaCl (pH 8.0). The hybridization buffer was a 10 mM phosphate buffer solution containing 0.1 M NaCl (pH 7.4).

2.2. Preparation of capture-probe-modified electrodes

To begin, gold electrodes (d = 2 mm) were polished using 1.0, 0.3 and 0.05 μm Al_2O_3 suspension respectively, and then intensively rinsed by ethanol and water under sonication. Electrodes were electrochemically cleaned in fresh 0.5 M H_2SO_4 solution by potential scanning between 0 and 1.6 V until a reproducible cyclic voltammogram was obtained. After being rinsed and dried with nitrogen, the cleaned electrodes were immediately dispensed with 4 μL immobilization buffer which contained capture probes (1 μM) at room temperature for 2 h. Then, the capture-probe-modified electrodes were washed by phosphate buffer, and subsequently treated with 0.5% BSA solution for 15 min.

2.3. Electrochemical measurements

Electrochemical experiments were conducted in a standard three-electrode electrochemical cell arrangement using a CHI660C electrochemical workstation (CHInstrument, USA). The electrochemical cell consisted of the DNA sensor working electrode, a platinum wire counter electrode, and a saturated calomel electrode (SCE).

Faradic impedimetric measurements were carried out in a 0.1 M KCl solution containing the $[Fe(CN)_6]^{3-/4-}$ redox probe (4 mM concentration of each component). Impedance spectra were obtained over the frequency range of 0.01–10,000 Hz at +0.18 V (vs SCE). The amplitude of the alternating voltage was 0.005 V. Experimental spectra, presented in the form of complex plane diagrams (i.e., Nyquist plots), were analyzed by nonlinear least-squares. The impedance (Z) is expressed in terms of a real (Z_{Re}) and an imaginary (Z_{Im}) component. In the Nyquist diagram, the semicircle diameter of EIS is equal to R_{ct}. The reported result for every electrode in this study was the mean value of three parallel measurements.

The surface density of DNA sequences was determined by the chronocoulometric method [18]. The chronocoulometric plots (charge vs. square root of time) of the DNA recognition surface were obtained in 10 mM Tris–HCl (pH 7.4) buffer. The cationic redox active ruthenium (III) hexamine ($[Ru(NH_3)_6]^{3+}$) (50 μM) was then introduced into the buffer solution and allowed to equilibrate for 1 min followed by chronocoulometric measurement. The surface coverage of $[Ru(NH_3)_6]^{3+}$ was calculated as the difference in the chronocoulometric intercepts in the absence and presence of $[Ru(NH_3)_6]^{3+}$ and converted to the DNA surface density using the relationship $\Gamma_{DNA} = \Gamma_0(z/m)N_A$, where Γ_{DNA} is the surface density of the DNA, Γ_0 is the surface coverage of $[Ru(NH_3)_6]^{3+}$, z is the charge of $[Ru(NH_3)_6]^{3+}$, m is the number of DNA bases, and N_A is Avogadro's number.

3. Results and discussion

3.1. Sensing strategy

The conventional electrochemical DNA hybridization EIS sensors can be described as (Fig. 1A): DNA hybridization on the electrode leads to a much more crowded surface than that covered by single-stranded DNA. Also, highly populated negative charges that arise from phosphates linking DNA bases of hybridized double-stranded DNA render the interface hostile to approaching $[Fe(CN)_6]^{3-/4-}$ ions, leading to the increase of the charge transfer resistance (R_{ct}) consequently [19]. Unfortunately, the change of the charge density and steric effect is limited during the hybridization on the high-density DNA recognition interface used in the conventional EIS biosensor. The signal, corresponding to the fractional change of the charge transfer resistance obtained upon hybridization, is often relatively small. Attachments of charged and/or bulky particles, and also enzymes have been used to amplify the charge transfer resistance [19–21]. However, these additional amplification steps increase the complexity and cost of the detection system.

As for the novel protocol, all processes contain three steps as follows (Fig. 1B): (1) a lodging layer of single strand DNA probes is established on gold surface by controlling the experimental conditions; (2) bovine serum albumin (BSA) is employed as blocking agent and at the same time protecting agent to maintain the conformation of the lodging layer; (3) in the presence of target DNA, pairing process via hydrogen bonds of bases on two complementary strands occurs. In this case, DNA bases desorb from the gold surface and are wrapped inside the helix, leading to free space on the electrode–solution interface [22]. These free space caused by DNA hybridization allow the redox-probe ($[Fe(CN)_6]^{4-/3-}$) transport freely to the gold surface and the charge transfer resistance decreased. Since the length of the single strand probe is much greater than its width, even few amount of the target sequence hybridized with the probe would lead to a significant change of the interfacial conformation and the charge transfer resistance (R_{ct}), conferring a unique advantage in this electrochemical approach.

As mentioned above, the conformation of the ssDNA recognition interface was the most important factor influencing the performance of the biosensor. In conventional EIS DNA biosensor, the ssDNA recognition interface was developed at low temperature with longer wait times, which led to the selective binding of thiol groups of the thiol-derivatized ssDNA probe onto the gold surface. Although the self-assemble monolayer (SAM) is constructed by packed standing ssDNA probes (7.52×10^{12} molecules/cm^2, measured by chronocoulometric method, see Table 2), the charge

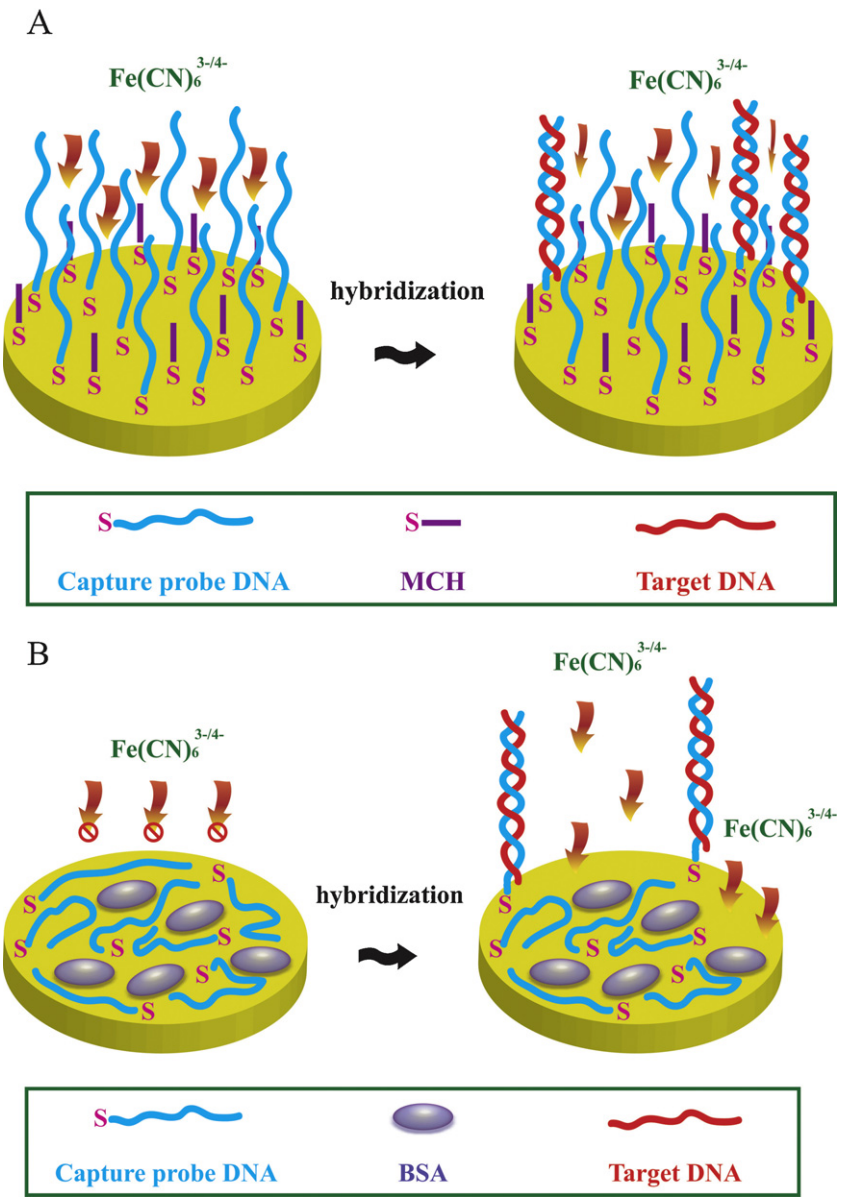

Fig. 1. Scheme of (A) the conventional EIS DNA biosensor and (B) the novel EIS DNA biosensor.

transfer resistance increases to small extend as compared to that of bare gold electrode (Fig. 2). This can be ascribed to the penetration of redox probes through the defects in the SAM. Since the nitrogen-containing nucleotide side chains can interact directly, strongly and rapidly with the gold surface [23,24], DNA recognition interface with lodging probes can be established by dispersed thiol-derivatized single-stranded DNA (ssDNA) probes on the gold surface at room temperature for 2 h. In this case, SH-ssDNA probes were tethered to the gold surface not only by S–Au bond but also by the interaction between bases and Au. Although the DNA surface density of this recognition interface is lower than that of conventional EIS DNA biosensor (3.22×10^{12} molecules/cm^2, measured by chronocoulometric method, see Table 2), the charge transfer resistance of this recognition interface was 37.6 kΩ, approximately ten times more than that of ssDNA SAM. According to the impedance variation (Fig. 3), the conformation of the SH-ssDNA probe on the gold surface is time dependent. In short time, the formation of the conformation is dominated by the kinetic process rather than thermodynamic process. Thus, a lodging conformation of conjugated ssDNA was formed due to the interaction between the gold surface and the base groups which obviously outnumbered the thiol

Table 2
DNA density on the electrode surface.

Electrode	DNA density (10^{12} molecules/cm^2)
Gold electrode modified by SH-ssDNA at 4 °C for 12 h (electrode 1)	7.52
Gold electrode modified by SH-ssDNA at 25 °C for 2 h (electrode 2)	3.22
Electrode 2 modified by MCH	3.04
Electrode 2 modified by BSA (electrode 3)	3.20
Electrode 2 after heating process	3.22
Electrode 3 after heating process	3.22

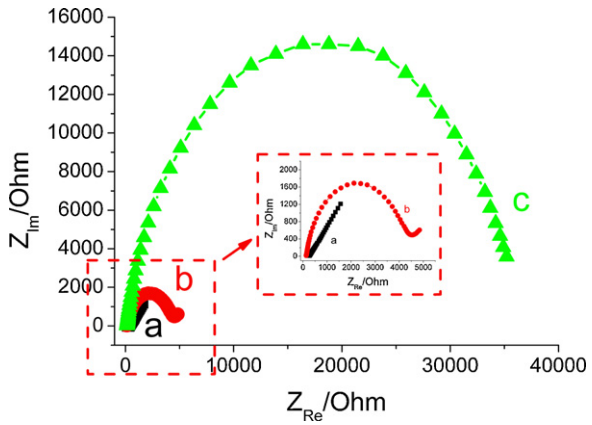

Fig. 2. Nyquist plots of bare gold electrode (a), gold electrode modified by SH-ssDNA at 4 °C for 12 h (b), and gold electrode modified by SH-ssDNA at 25 °C for 2 h (c).

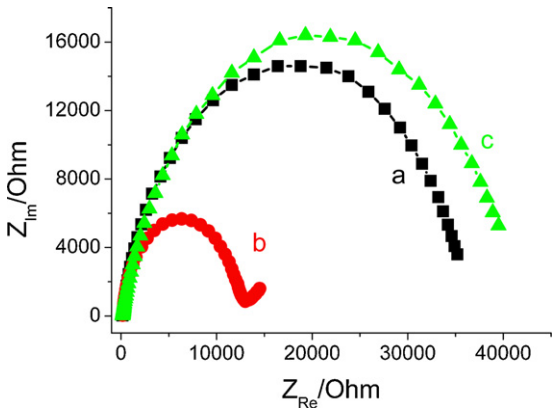

Fig. 4. Nyquist plots of the ssDNA-modified gold electrode (a), ssDNA-modified gold electrode passivated by MCH (b), and ssDNA-modified gold electrode passivated by BSA (c).

groups in a same SH-ssDNA molecule. However, long-time exposure to the solution of SH-ssDNA probe results in the displacing of adsorbed DNA bases by thiol groups of other probes from the solution, which has a stronger interaction with gold than nitrogen.

In order to reduce the defects in the recognition layer, blocking agent was introduced to fill the unoccupied gold sites. However, the most common blocking agent, mercaptohexanol (MCH), is not suitable for our recognition interface. As an alkanethiol, MCH not only occupied exposed gold sites but also replaced the binding between gold and DNA bases, leading to the orientational transformation of the ssDNA probes. The MCH post-treatment makes the ssDNA molecules raised off the gold surface to form a conformation where they are bound to the gold surface solely by the sulfur atom [22,23]. Alternatively, bovine serum albumin (BSA), which will not replace the base binding, were chosen in our experiment to eliminate the defects in the recognition layer. As expected, the impedance increased slightly after the passivation by BSA, suggesting that BSA maintained the lodging conformation of the ssDNA layer (Fig. 4). In order to verify the influence of the temperature on the conformation of the recognition interface, both the ssDNA/BSA and ssDNA modified electrodes were incubated under the hybridization temperature in the buffer solution. In the case of ssDNA modified electrode (Fig. 5), the impedance decreased dramatically after heated in the hybridization buffer solution. This fact suggested that a significant amount of bound DNA bases were untethered from the gold surface since the DNA density on the electrode kept almost unchanged during the heating process due to the relatively thermal stable S–Au interaction (see Table 2). However, when the ssDNA/BSA modified electrode was heated in the hybridization buffer solution, a totally different result was observed, which the impedance value slightly increased rather than decreased during the heating process. This interesting result indicated that the lodging conformation of ssDNA probe might be further stabilized by BSA during the heating process.

3.2. The sensitivity and selectivity of designed sensing system

The sensitivity of the designed biosensor was investigated by testing the sensory responses at different concentrations of the complementary target DNA. As shown in Fig. 6A, the impedance value decreased with the increasing concentration of complementary sequence. The analytical signal, R_{ct}, had a linear relationship with the logarithmic value of the target DNA concentration ranging from 1.0×10^{-13} to 1.0×10^{-8} M (Fig. 6B). The regression equation was $R_{ct}(\Omega) = 36306.6 - 7366.1 \log C_{DNA}$ (pM), with a correlation coefficient of 0.9995. The detection limit was experimentally found to be 40 fM using 3σ, where σ was the standard deviation of the blank solution with 10 parallel measurements. The sensitivity of the biosensor is superior to other types of EIS DNA biosensors (3.5 nM [19]; 3.8 pM [25]; 0.5 nM [26]; 1 nM [27]; 0.01 nM [28]). The impedance variation of the biosensor is consistent with the amount of hybridized DNA measured by chronocoulometric method (Fig. 7).

To evaluate the selectivity of the biosensor, different DNA sequences with the same concentration of 10 nM were used to hybridize with the probe ssDNA immobilized on the electrode. As shown in Fig. 8, a significant decrease in the R_{ct} value was observed for target DNA, which corresponded to the hybridization of the probe ssDNA with a fully complementary sequence.

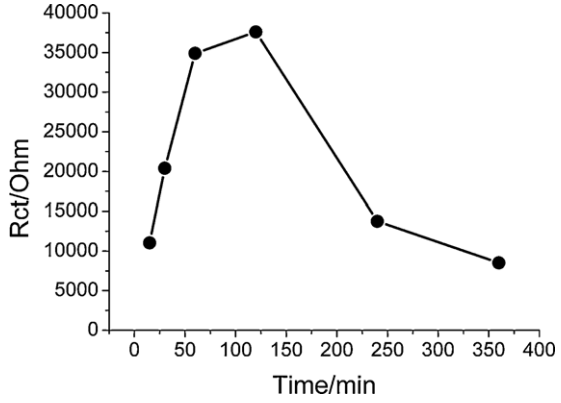

Fig. 3. Charge transfer resistance of the gold electrode modified by SH-ssDNA with different time.

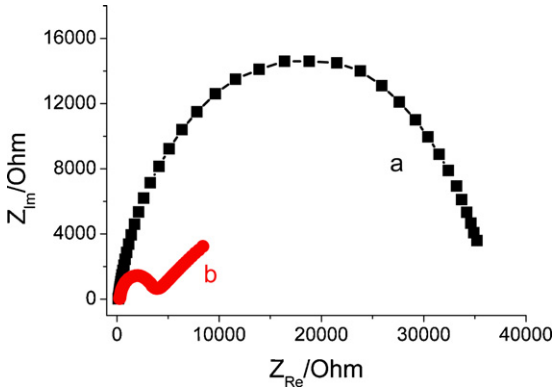

Fig. 5. Nyquist plots of the ssDNA-modified gold electrode before (a) and after (b) incubated at 37 °C for 40 min in the hybridization buffer solution.

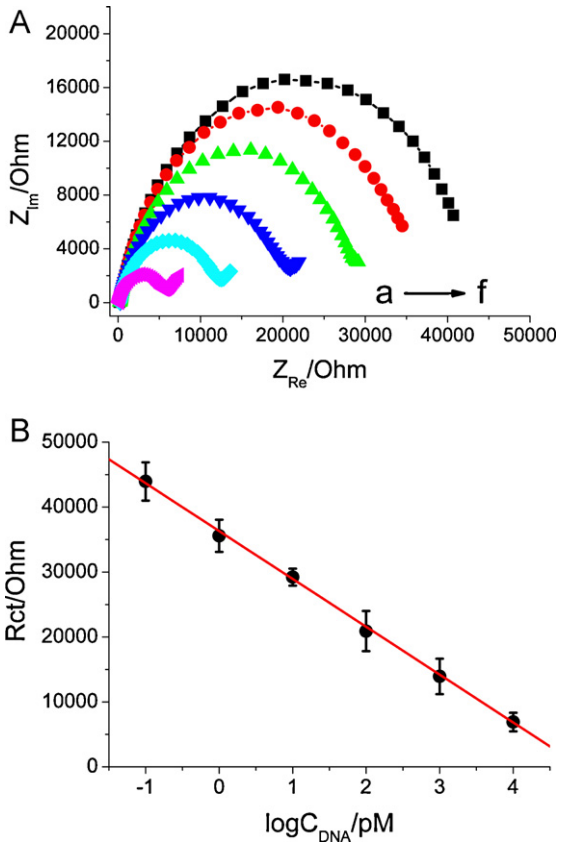

Fig. 6. (A) Nyquist plots of BSA/ssDNA/AuE after hybridization (37 °C, 40 min) with its complementary PML/RARα fusion gene sequence of different concentrations: 10 nM (a), 1 nM (b), 100 pM (c), 10 pM (d), 1 pM (e), and 100 fM (f). (B) The plot of R_{ct} versus complementary DNA concentration.

Nevertheless, only negligible decrease in the R_{ct} value was observed for non-complementary sequences. Moreover, when the salmon sperm DNA was used as long-sequence negative control, the measured impedance was close to the result of a blank experiment. These results clearly demonstrated that the designed sensor was essentially insensitive to non-matched DNA sequences, regardless of the length of the sequence. Furthermore, in order to confirm whether or not the observed impedance variation arises from DNA hybridization, the electrode mentioned above was subsequently re-hybridized with fully complementary sequence. The resulting impedance spectra turned out to be nearly the same as that

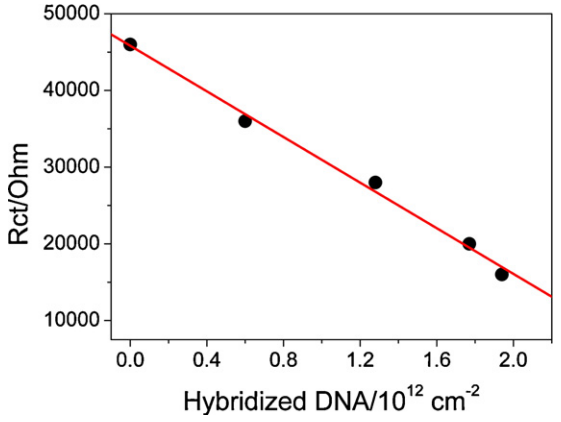

Fig. 7. Relationship between the impedance of the biosensor and the amount of hybridized DNA.

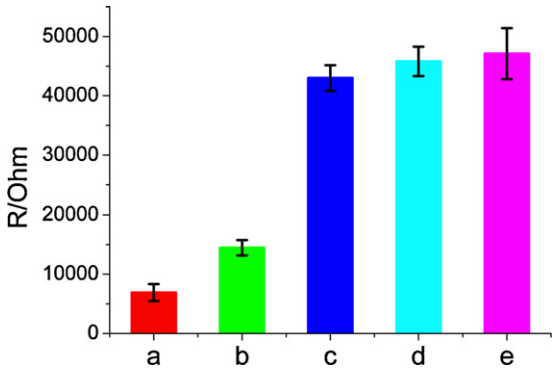

Fig. 8. The histograms of R_{ct} signals at BSA/ssDNA/Au after hybridization with complementary target DNA sequence (a), one-base mismatch DNA sequence (b), salmon sperm DNA (c), non-complementary DNA sequence (d), and hybridization buffer solution (e).

corresponding to the hybridization with fully complementary sequence. One-base mismatch sequence was also investigated and the R_{ct} value was shown as Fig. 8. The result showed that the difference between one-base mismatch sequence and complementary sequence was obvious. These results confirmed that the ssDNA/BSA modified electrode fabricated in this study had high selectivity.

4. Conclusions

In summary, we have demonstrated a novel approach of utilizing the conformational change from a random coil lying structure of ssDNA to a rigid standing chain of double-stranded DNA (dsDNA) to recognize DNA hybridization by AC impedance method. The success for this study lies on the lodging conformation of SH-ssDNA probes immobilized on the gold electrode. Another key component in the determination is that BSA can block the exposed gold sites and at the same time maintain the lodging structure of unhybridized ssDNA probes on the recognition interface. Even without any amplification protocol, this facile approach is much more sensitive than the conventional EIS DNA biosensors. Moreover, the reported sensor achieves impressive selectivity with successful discrimination of the target DNA from various mismatch sequences. The simple strategy described here is thus expected to be promised for a wide range of nucleic acid testing, including clinical diagnostics, food safety, biothreat detection, and forensic analysis.

Acknowledgments

The authors gratefully acknowledge the financial support of the National High Technology and Development of China (863 Project: 2008AA02Z433), the National Natural Science Foundation of China (20805006, 20975021, 21175023), the Fujian Provincial University-Industry Cooperation Science & Technology Major Program (2010Y4003), the Foundation of Fujian Key Laboratory of Hematology (2009J1004), the Scientific Research Major Program of Fujian Medical University (09ZD013), the Medical Innovation Project of Fujian Province (2009-CX-17), the Program for New Century Excellent Talents in Fujian Province University (W. Chen), Science and Technology Planning Project of Fujian Province (2011Y0030), and Excellent Youth Talent Program of the Fujian Province University (JA10126).

References

[1] T.G. Drummond, M.G. Hill, J.K. Barton, Nat. Biotechnol. 21 (2003) 1192–1199.
[2] A. Sassolas, B.D. Leca-Bouvier, L.J. Blum, Chem. Rev. 108 (2008) 109–139.
[3] F. Patolsky, A. Lichtenstein, I. Willner, Nat. Biotechnol. 19 (2001) 253–257.
[4] J. Zhang, S. Song, L. Wang, D. Pan, C. Fan, Nat. Protoc. 2 (2007) 2888–2895.

[5] Y. Xiao, R.Y. Lai, K.W. Plaxco, Nat. Protoc. 2 (2007) 2875–2880.
[6] C. Fan, K.W. Plaxco, A.J. Heeger, Proc. Natl. Acad. Sci. U.S.A. 100 (2003) 9134–9137.
[7] J. Wang, G. Liu, A. Merkoçi, J. Am. Chem. Soc. 125 (2003) 3214–3215.
[8] F. Patolsky, A. Lichtenstein, M. Kotler, I. Willner, Angew. Chem. Int. Ed. 40 (2001) 2261–2265.
[9] M.J.A. Shiddiky, A.A.J. Torriero, Z. Zeng, L. Spiccia, A.M. Bond, J. Am. Chem. Soc. 132 (2010) 10053–10063.
[10] Y. Zhang, Y. Wang, H. Wang, J.H. Jiang, G.L. Shen, R.Q. Yu, J. Li, Anal. Chem. 81 (2009) 1982–1987.
[11] J. Zhang, S. Song, L. Zhang, L. Wang, H. Wu, D. Pan, C. Fan, J. Am. Chem. Soc. 128 (2006) 8575–8580.
[12] F. Xia, R.J. White, X. Zuo, A. Patterson, Y. Xiao, D. Kang, X. Gong, K.W. Plaxco, A.J. Heeger, J. Am. Chem. Soc. 132 (2010) 14346–14348.
[13] Y. Xiao, X. Lou, T. Uzawa, K.J.I. Plakos, K.W. Plaxco, H.T. Soh, J. Am. Chem. Soc. 131 (2009) 15311–15316.
[14] J. Wu, S. Campuzano, C. Halford, D.A. Haake, J. Wang, Anal. Chem. 82 (2010) 8830–8837.
[15] A. Bogomolova, E. Komarova, K. Reber, T. Gerasimov, O. Yavuz, S. Bhatt, M. Aldissi, Anal. Chem. 81 (2009) 3944–3949.
[16] X. Jiang, M.G. Spencer, Biosens. Bioelectron. 25 (2010) 1622–1628.
[17] A. Bonanni, M. Pumera, ACS Nano 5 (2011) 2356–2361.
[18] A.B. Steel, T.M. Herne, M.J. Tarlov, Anal. Chem. 70 (1998) 4670–4677.
[19] A. Bardea, F. Patolsky, A. Dagan, I. Willner, Chem. Commun. (1999) 21–22.
[20] F. Patolsky, A. Lichtenstein, I. Willner, Angew. Chem. Int. Ed. 39 (2000) 940–943.
[21] F. Patolsky, E. Katz, A. Bardea, I. Willner, Langmuir 15 (1999) 3703–3706.
[22] J.N. Murphy, A.K.H. Cheng, H.Z. Yu, D. Bizzotto, J. Am. Chem. Soc. 131 (2009) 4042–4050.
[23] T.M. Herne, M.J. Tarlov, J. Am. Chem. Soc. 119 (1997) 8916–8920.
[24] G. Liu, C. Sun, D. Li, S. Song, B. Mao, C. Fan, Z. Tian, Adv. Mater. 22 (2010) 2148–2150.
[25] A. Li, F. Yang, Y. Ma, X. Yang, Biosens. Bioelectron. 22 (2007) 1716–1722.
[26] X. Liu, X. Qu, J. Dong, S. Ai, R. Han, Biosens. Bioelectron. 26 (2011) 3679–3682.
[27] S.D. Keighley, P. Estrela, P. Li, P. Migliorato, Biosens. Bioelectron. 24 (2008) 906–911.
[28] B. Kannan, D.E. Williams, M.A. Booth, J. Travas-Sejdic, Anal. Chem. 83 (2011) 3415–3421.